9. R. L. Abrams, IEEE J. Quantum Electron. QE-8, 838 (1972).
10. W. T. Welford, *Aberrations of the Symmetrical Optical System* (Academic, New York, 1974), pp. 198–199.
11. W. J. Tomlinson, R. E. Wagner, T. S. Stakelon, T. W. Cline, R. B. Jander, in *Technical Digest, Third International Conference IOOC* (Optical Society of America, Washington, D.C., 1981), paper TuL2; R. E. Wagner and W. J. Tomlinson, "Coupling Efficiency of Optics in Single-Mode Fiber Components," to be published.

## Easier way to find the sagittal depth: comments

Berlyn Brixner

University of California, Los Alamos National Laboratory, Los Alamos, New Mexico 87545.
Received 2 November 1981.

A recent Letter by Foote[1] presented formulas for calculating the exact and approximate sagittal depth of a chord. Although the formula is correct, the accuracy claimed for the approximate formula (one part in 2000 for $d = R/4$) is not obtained. We present here a single, simple, and easily remembered formula for calculating both the approximate and, by iteration, the exact sagittal depth.

$$s = r^2/(2R - s),$$

where $r$ is one-half of the chord length, and $R$ is the circular radius of curvature. When the $s$ in the denominator is set at zero, one obtains an approximate formula equivalent to that given by Foote.

**Table I. Calculation of Sagittal Depths for $R = 100$**

| Iteration | Calculated sagittal depths for chord length 20 | 40 | 80 | 120 |
|---|---|---|---|---|
| 1 | 0.500000 | 2.000000 | 8.000000 | 18.000000 |
| 2 | 0.501253 | 2.020202 | 8.333333 | 19.780219 |
| 3 | 0.501256 | 2.020408 | 8.347826 | 19.975609 |
| 4 | 0.501256 | 2.020410 | 8.348458 | 19.997090 |
| 5 | | 2.020410 | 8.348485 | 19.999698 |
| 6 | | | 8.348486 | 19.999966 |
| 7 | | | 8.348486 | 19.999996 |
| 8 | | | | 20.000000 |
| 9 | | | | 20.000000 |

Table I gives the successive approximations of the sagittal depth for several chord lengths in a circle with $R = 100$. The first entry is the depth given by the approximate formula ($s$ in the denominator set at zero). In most cases, the calculation accuracy is seen to progress at about one significant figure per iteration. The increasingly accurate sequence of sagittal approximations makes it easy to detect errors in the arithmetic. Note that the approximate formula makes an error of about one part in 400 when the chord length is $R/5$, much greater than claimed by Foote.

This work was performed under the auspices of the U.S. Department of Energy, under contract W7405-ENG-36.

### Reference

1. V. S. Foote, Appl. Opt. 20, 2605 (1981).

## Photon correlation spectroscopy used as a particle size diagnostic in sooting flames

Galen B. King, C. M. Sorensen, T. W. Lester, and J. F. Merklin

All authors are with Kansas State University, Manhattan, Kansas 66506; C. M. Sorensen is in Department of Physics, the others are in Department of Nuclear Engineering.
Received 31 August 1981.
0003-6935/82/060976-03$01.00/0.


Light-scattering particulate size measurements in flames have several advantages over conventional probe sampling. These include negligible perturbation of the system, real-time analysis, and *in situ* measurement of the particle sizes. The two techniques widely used today, Mie scattering and the extinction ratio method, rely on an accurate knowledge of the refractive index of the particulate matter in the flame. This refractive index is poorly known in most cases, its dependence on chemical composition is unknown, and it cannot be determined *in situ*. Photon correlation spectroscopy (PCS), a light-scattering technique with the above advantages, does not rely on the particulate refractive index. In this Letter we demonstrate this technique's feasibility for particulate size determination in flames.

The basic theory of the method was developed by Benedek[1] and Cummins and Swinney.[2] Consider a system of particles of radius $r$ suspended in a fluid of viscosity $\eta$ traveling in a laminar flow field with velocity $\mathbf{v}$. For a large incident beam the normalized scattered-light correlation function is

$$C(\mathbf{K},t) = \exp(i\mathbf{K}\cdot\mathbf{v})\exp(-DK^2t) + B, \quad (1)$$

where $B$ is a noise or background term, $t$ is time, $\mathbf{K}$ is the scattering wave vector whose magnitude is

$$|\mathbf{K}| = (4\pi n/\lambda)(\sin\theta/2), \quad (2)$$

and $D$ is the hydrodynamic diffusion constant given by

$$D = k_BT/6\pi\eta r. \quad (3)$$

In Eqs. (2) and (3) $n$ is the refractive index of the medium, $\lambda$ is the wavelength of the incident light, $\theta$ is the scattering angle, $k_B$ is Boltzmann's constant, and $T$ is the temperature.

The hydrodynamic or Stokes-Einstein diffusion constant may not hold for particle sizes less than the mean free path of the gas molecules in the flame, $r < \lambda$. In a 1500 K atmospheric pressure flame the mean free path is $\lambda \simeq 3000$ Å, and soot particles sized less than this are quite common. Thus, a more realistic kinetic form for the diffusion constant may be necessary, especially in the extreme $r \ll \lambda$ region. It is not clear at this time, however, what the proper form of the diffusion constant is in the region intermediate between these two limits, kinetic and hydrodynamic. Until this problem is resolved we shall, in what follows, use the hydrodynamic result of Eq. (3). The results of our experiment are unaffected by this problem except for the possibility of modifying the particulate sizes.

The desired particulate size information is contained in the diffusion constant $D$ involved in the second factor on the right-hand side of Eq. (1). It is desirable to make the first factor, the Doppler term due to the flow velocity of the particle, as unimportant as possible. This is done by adjusting the scattering plane perpendicular to the flow velocity; i.e., (ideally) $\mathbf{K}\cdot\mathbf{v} = 0$. In practice, however, because of finite

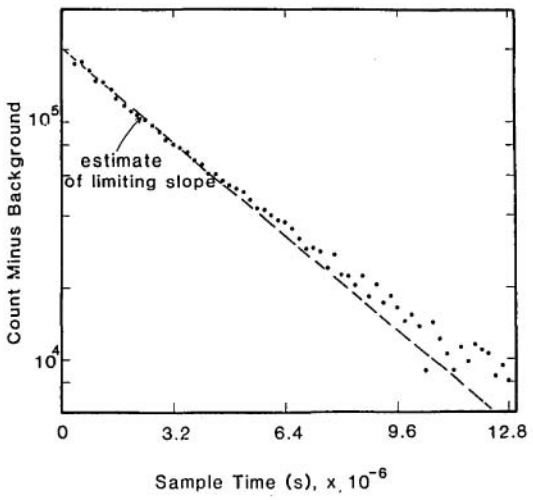


Fig. 1. A semilogarithmic plot of the counts per channel minus background vs the sample time for a typical photon correlation spectrum from particles in the flame.

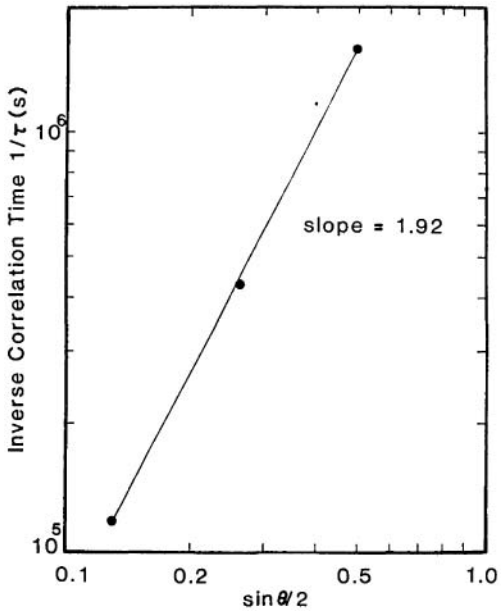


Fig. 2. The inverse correlation time vs $\sin\theta/2$ where $\theta$ is the scattering angle.

incident and collection angle uncertainties, this condition is not completely attainable. For an incident beam with a Gaussian profile of width $\sigma$ the scattered-light correlation function in the homodyne mode is

$$C(\mathbf{K},t) = \exp(-v^2t^2/4\sigma^2)\exp(-2DK^2t) + B. \quad (4)$$

By adjusting the beamwidth the first factor can be made relatively constant over the correlation time $\tau_c = 1/(2DK^2)$ so that particle radius may be determined.

Earlier work using dynamic light scattering by Bernard and Penner[3] used an analog power spectra method to determine particle size in an ethylene–oxygen flame. PCS uses digital methods to determine the correlation function of the scattered light, the Fourier transform of the power spectrum. PCS is both more photon efficient and has lower noise.

From a temperature measurement and Lennard-Jones parameters the viscosity may be calculated and the particulate radius determined from the correlation time. As a rule the viscosity of gases is a function of temperature to the 0.7–0.8 power, but in Eq. (3) $T/\eta$ is calculated and thus a fair error in temperature measurement will not cause as great an error in the calculated particle size.

To test PCS use in flames, a simple wick flame was employed. Light from an Ar-ion laser operating at 488 nm was focused into the flame. Scattered light passed first through a 10-nm bandpass filter to minimize blackbody radiation, then through a pinhole, and was detected in the homodyne mode by an ITT FW130 photomultiplier tube (PMT). The photopulses were amplified and discriminated and then passed to a digital correlator. The detector housing and PMT were mounted on an optical rail which pivoted about the center of the scattering volume so as to form a goniometer. The wick flame was an ornamental lantern and the fuel was commercial lamp oil of composition 99% kerosene. The lantern was placed on a translation table; thus the flame could be probed at various positions.

A typical spectrum of the experimental correlation function minus the background vs time is shown in Fig. 1. The exponential nature of the data as predicted by Eq. (4) is clearly seen. The slope of this line in the limit $t \to 0$, is the inverse correlation time. The deviation from linearity in Fig. 1 could be caused by two factors. From Eq. (4) the instrumental profile factor has a $t^2$ dependence in the exponent. This term can be thought of equivalently as either a measure of the time for a particle to cross the beam or a measure of the convergence and divergence of the incident and scattered light.[4] Secondly, this deviation from linearity could be caused by a size distribution in the particles causing the scattering.[5]

Figure 2 is a log–log plot of the inverse correlation time vs $\sin\theta/2$ for three different experimental angles. These data have a slope of 1.92 compared with the expected value of 2 [from Eq. (2) and (4)]. The agreement between experiment and theory indicates that the detected light was indeed scattered from diffusing particles.

To measure the temporal stability of the flame fifteen spectra were taken at 30-min intervals. The percent standard deviation in slopes of the correlation function from these spectra was <0.1%. Three positions were chosen and spectra alternately collected until there were five spectra at each point to test repeatability. The percent standard deviation was 1%; therefore, any location in the flame could be probed with reasonable precision.

**Table I. Particle Diameters and Associated Correlation Times as a Function of Position in a Wick Flame**

| | Height (cm) | Radius (cm) | Correlation time ($\times 10^{-6}$ sec) | Diameter (nm) |
|---|---|---|---|---|
| 1 | 1.143 | 0.0 | 2.57 | 9.0 |
| 2 | 1.397 | 0.0 | 3.30 | 11.7 |
| 3 | 1.651 | 0.0 | 4.01 | 14.2 |
| 4 | 1.905 | 0.0 | 4.31 | 15.2 |
| 5 | 2.032 | 0.0 | 3.89 | 13.6 |
| 6 | 1.778 | 0.0 | 4.24 | 15.0 |
| 7 | 1.524 | 0.0 | 3.65 | 12.9 |
| 8 | 1.270 | 0.0 | 2.97 | 10.5 |
| 9 | 1.016 | 0.0 | 2.31 | 8.2 |
| 10 | 1.143 | 0.0 | 2.47 | 8.7 |
| 11 | 1.143 | 0.025 | 2.52 | 8.9 |
| 12 | 1.143 | 0.051 | 2.77 | 9.8 |
| 13 | 1.143 | 0.076 | 2.99 | 10.6 |
| 14 | 1.143 | 0.102 | 3.42 | 12.1 |
| 15 | 0.889 | 0.127 | 3.03 | 10.7 |

Shown in Table I are the correlation times at the listed location for particles in this flame. Correlation times vary, as would be expected, both vertically and horizontally for this flame. The temperature was measured to be ~1300 K with an uncoated thermocouple. With this information the viscosity was calculated and in turn particle size was determined. In Fig. 3 particle diameter vs height above the base of the wick is plotted. Particle diameters vary from 8–15 nm. Particles increase in size until shortly before the end of the luminous region at which point the size decreases. No soot could be seen leaving the flame, and thus this type of distribution would be expected due to particle burnout in the flame. The absolute values of the particle sizes could change depending on the poorly measured temperature, but the relative size and size vs height distribution of the particles will remain the same.

Although this wick flame is crude, data from it demonstrate that PCS is a viable technique for use in flames. This technique is independent of the particulate refractive index, it has

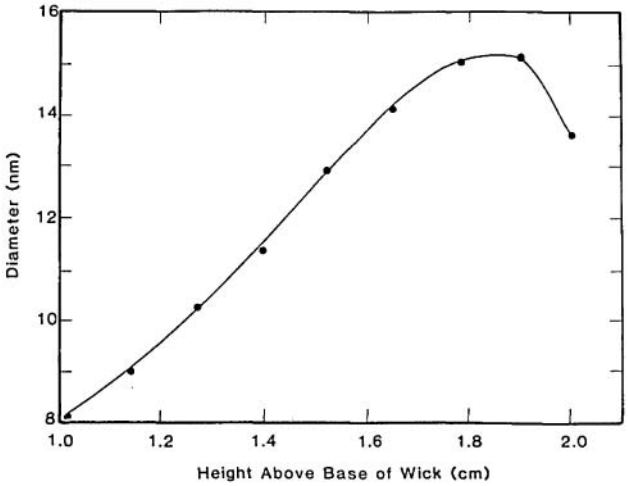


Fig. 3. Variation of soot particle diameters with height above the base of the burner.

proved to be of high precision, and it has accuracies comparable with measurements made by other techniques.[6] With refinement this technique should yield information on particle growth rates, shape, and velocities in flames as it has in other fields.

The authors acknowledge the support of the Department of Energy, Division of Chemical Sciences, which is supporting this research under contract DE-AC02-80ER10677.

## References

1. G. B. Benedek, *Polarization, Matter, and Radiation* (Presses Universitaires de France, Paris, 1969), p. 49.
2. H. Z. Cummins and H. L. Swinney, Prog. Opt. **8**, 135 (1970).
3. J. M. Bernard and S. S. Penner, Prog. Astronaut Aeronaut. **53**, 411 (1976).
4. R. V. Edwards, J. C. Angus, M. J. French, and J. W. Dunning, Jr., J. Appl. Phys. **42**, 837 (1971).
5. D. E. Koppel, J. Chem. Phys. **57**, 4814 (1972).
6. G. P. Prado, M. L. Lee, R. A. Hites, D. P. Hoult, and J. B. Howard, in *Proceedings, Sixteenth International Symposium on Combustion* (Combustion Institute, Pittsburgh, 1977), p. 649.

# Wave slope statistics derived from optical radiance measurements below the sea surface

L. B. Stotts and S. Karp

Larry Stotts is with U.S. Department of Navy, Naval Ocean Systems Center, San Diego, California 92152, and S. Karp is with Defense Advanced Research Projects Agency, Strategic Technology Office, Washington D.C. 20009.

Received 27 October 1981.

The directional nature and intensity of optical radiation reflected and refracted at the air–sea interface depends on the effective slope of the particular element of sea surface illuminated at that instant of time.[1–3] Waves and swells of all wavelengths down to the shortest capillary waves, as well as bubbles, spume, and detritus, combine to create resultant radiance distributions, many times causing the focusing and dispersing of small bundles of light rays. In general, though, the slopes and curvatures of the sea surface involved in the above are controlled by the smaller wavelength waves and ripples created by the wind.[4–6] The mean square and probability distributions of these slopes have been measured and correlated with wind speed in the open ocean by Cox and Munk[4,6,7] and Schooley.[5] In particular, the former authors showed these slopes to have mean square variances which vary linearly with wind speed and a probability distribution given by a Gram-Charlier series.[4–6] However, Wu reanalyzed their cited data and showed the mean square slopes to actually vary logarithmically in wind speed within two distant regions of wave generation rather than linearly in a continuous fashion.[8,9]

Comparisons have been made between the above models and some experimental data.[10–14] Cox,[10] Wu,[11] Bobb *et al.*,[12] and Palm *et al.*[13] have measured mean square slope variances and probability distribution within controlled laboratory conditions, and Cox,[10] Wu,[11] and Schau[14] have measured these characteristics in the open ocean environment. The laboratory experiments have shown larger slope variances than anticipated by laboratory predictions consistently,[15] while the limited oceanic data appear in reasonable agreement.[9] The smaller wave slopes measured in the open ocean have been attributed, at least in part, to the suppression of capillary wave growth by gravity waves, an aspect the laboratory experiments were not subject to.[15] This Letter reports a new technique for measuring wave slope distributions *in situ* which is both inherently simpler to implement than previously utilized methods[10–15] and totally noninterfering to the wave generation process.[14] A preliminary result obtained using the technique in the field is that the Cox and Munk/Wu models may indeed underestimate mean wave slope variances as first suggested by Bobb *et al.*[12] by as much as a factor of 2 in our particular experimental scenario. This will be discussed in more detail shortly.

The basis for the wave slope measurement technique is that each facet of a randomly ruffled ocean surface will uniquely deviate a collimated radiance distribution from its initial incident direction independent of the slope distributions about it.[2,3] Thus, the time-averaged radiance of a collimated plane wave source just below the air–sea interface is directly proportional to the probability density function of wave slopes for illumination angles near zenith.[2–4] This fact suggests a very simple means of acquiring wave slope statistics in the field; namely, by making solar radiance measurements at very shallow depths on clear sunny days. This technique was employed during the summer of 1975.